IOP Publishing Journal of Physics D: Applied Physics
J. Phys. D: Appl. Phys. **49** (2016) 085101 (6pp) doi:10.1088/0022-3727/49/8/085101

Temperature dependent electrical characterization of thin film $Cu_2ZnSnSe_4$ solar cells

E Kask[1], J Krustok[1], S Giraldo[2], M Neuschitzer[2], S López-Marino[2] and E Saucedo[2]

[1] Tallinn University of Technology, Ehitajate tee 5, 19086 Tallinn, Estonia
[2] Catalonia Institute for Energy Research, IREC, Jardins de les Dones de Negre 1, 08930 Sant Adrià del Besòs, Barcelona, Spain

E-mail: erkki.kask@ttu.ee

Received 16 August 2015, revised 15 November 2015
Accepted for publication 18 November 2015
Published 25 January 2016

Abstract

Impedance spectroscopy (IS) and current–voltage characteristics measurements were applied to study properties of a $Cu_2ZnSnSe_4$ (CZTSe) thin film solar cell. IS measurements were done in the frequency range 20 Hz to 10 MHz. The measurement temperature was varied from 10 K to 325 K with a step $\Delta T = 5$ K. Temperature dependence of V_{oc} revealed an activation energy of 962 meV, which is in the vicinity of the band gap energy of CZTSe and hence the dominating recombination mechanism in this solar cell is bulk recombination. Different temperature ranges, where electrical properties change, were found. Interface states at grain boundaries with different properties were revealed to play an important role in impedance measurements. These states can be described by introducing a constant phase element in the equivalent circuit.

Keywords: $Cu_2ZnSnSe_4$, impedance spectroscopy, current–voltage characteristics, grain boundaries

(Some figures may appear in colour only in the online journal)

1. Introduction

Quaternary compound $Cu_2ZnSnSe_4$ (CZTSe) with a direct band gap and high absorption coefficient ($>10^4$) [1] is a promising absorber material for photovoltaics. Moreover, CZTSe is a low-cost non-toxic semiconductor material, whose elemental constituents are abundant in the Earth's crust. The current power conversion efficiency record of a CZTSe device is 11.6% [2]. Photovoltaic performance is hindered by a large variety of intrinsic lattice defects, which have influence on optical and electrical properties of solar cells. Little information about the defect structure of CZTSe can be found in the literature.

Defects have been studied by photoluminescence spectroscopy [3–6] and also by capacitive spectroscopy methods. In our previous works [7, 8] we studied so-called monograin solar cells consisting of a microcrystal absorber material, and different defect levels were detected. In CZTSe two defect states were observed by admittance spectroscopy (AS). The unstable defect state showed activation energies from 87 meV to 100 meV and was attributed to the interface states because the possible change of interface properties with time could alter activation energy. The second state at 74 meV was assumed to belong to Cu_{Zn}^{-}. These activation energies were found by measuring impedance Z and phase angle θ versus frequency f, and calculating capacitance C by employing an equivalent circuit, where a series resistor R_s is followed by a resistor R_p and a capacitor connected in parallel, (R_s and R_p cover series resistance of a structure, wires, contacts, etc, and shunt resistance of the junction, accordingly). Inverse temperature versus the natural logarithm of angular frequencies ω that correspond to a capacitance step showed linear dependence and this was used for activation energy calculation.

Weiss *et al* [9] have studied modelling equivalent circuit responses in kesterite solar cells and found that the evaluation of the admittance data cannot be performed simply with the as-measured capacitance data, as an increasing series resistance with decreasing temperature results in a capacitance step within the *C–f* profile. For instance, they suppose that measurements data need to be discarded at higher frequencies and at lower temperatures. In addition, they used current–voltage characteristics (*I–V*) to extract series and shunt resistances, but resistances found by direct current measurements are not perfectly suitable for replacing resistance values of alternating current measurements. Moreover, they used as-measured capacitance (meaning no series resistance exists) and later applied series resistance to it.

Goodman [10] showed that accurate measurement of capacitance requires both $R_s \ll R_p$ and $R_s \ll (\omega C)^{-1}$ so that the capacitive impedance is the dominant circuit element. Ordinarily, the quantity C is assumed to be frequency independent, but in experiments this is not always true; reasons may be, for example, charge relaxation times. In general, such effects tend to disappear with increasing frequency and may place a lower limit on the trustworthy frequency range. Moreover, limitations with respect to measurement equipment may place further restrictions upon the measurement frequency. These restrictions require that the resistance and geometry of the solar cell are suitably chosen.

Fernandes *et al* [11] have studied AS of Cu_2ZnSnS_4 (CZTS) solar cells and also applied various equivalent circuits to fit measured data. They calculated the deviation between measured and fitted data and found that their fitting of measured data is satisfsctory only via a quite complicated model. Usually, the more elements used in an equivalent circuit the better fit found, but in this case the interpretation is impossible or inappropriate. Moreover, Friesen *et al* [12] studied a thin film CdTe solar cell and state that as commonly applied equivalent circuit models consist only of frequency-independent circuit elements they cannot be used to describe the frequency dispersion of a thin film solar cell. They replaced the capacitor with a frequency-dependent non-ideal capacitor, called the constant phase element (CPE). It is generally assumed that non-ideal capacitance behaviour originates from a distribution in the current density due to material inhomogeneity and/or the grain boundaries [12]. The use of a CPE provides a better fitting for a depressed semicircle in the Nyquist plot.

According to our previous temperature-dependent measurements [13], three different temperature ranges, where electrical parameters change, were seen in monograin CZTS solar cells. At very low temperatures ($T < 40$ K) the effective band gap energy E_g^* and series resistance R_s showed steep changes and this behaviour was interpreted as hole blocking at a CZTSe/CdS heterojunction. Therefore the interface recombination rate turns out to be very low at $T < 40$ K.

Usually, impedance spectroscopy (IS) and AS measurements are conducted at higher temperatures because models are then more easily applied and understood. Unfortunately, at very low temperatures interpreting IS spectra is quite difficult. In this work, we analyze this complicated IS measurements data at very low temperatures and correlate with grain boundaries properties. Also, IS measurements frequency range limits are shown and results of *I–V* measurements and IS for a CZTSe thin film solar cell are presented and analyzed.

2. Experiment

A CZTSe absorber for this study was prepared by reactive thermal annealing of a metallic Cu/Sn/Cu/Zn precursor stack deposited by dc magnetron sputtering onto Mo-coated soda lime glass substrates, as described elsewhere in more detail [14]. The CZTSe absorber composition was measured by x-ray florescence spectroscopy showing cation ratios of Cu/(Zn + Sn) = 0.69, Zn/Sn = 1.45, Cu/Zn = 1.16 and Cu/Sn = 1.69. The details of the preparation of the thin film solar cell device are given in [15]. The individual solar cell (with dimensions $3 \times 3\,\mathrm{mm}^2$) used for this study shows power conversion efficiency of $\eta = 6.6\%$ with $J_{sc} = 27.2$ mA cm^{-2}, $V_{oc} = 383$ mV and $FF = 64\%$.

For temperature-dependent measurements the selected thin film solar cells were mounted in a closed-cycle He cryostat (Janis). *I–V* curves were recorded using a Keithley SourceMeter 2401 with 100 mW cm^{-2} illumination. For a light source a standard 250 W halogen lamp with calibrated intensity was used. The impedance spectra curves were recorded using a Wayne Kerr 6500B impedance analyzer. For IS the impedance Z and phase angle θ were both measured as functions of frequency f and temperature T. The temperature was varied from 10 K to 300 K with a step $\Delta T = 5$ K. The used frequency was in the range 20 Hz to 10 MHz. In order to maintain the linearity of the response signal, the ac voltage was kept as low as 10 mV. The ac measurements were carried out in the dark and dc biases of 0 V and −0.5 V were used. After each measurement, the real and imaginary parts of the impedance, Z' and $-Z''$ respectively, were calculated. Measured data were fitted using the ZView (Scribner, USA) computer program, which gives values for elements used in an equivalent circuit; for example, series resistance, R_s.

3. Results and discussion

The studied solar cell exhibited an efficiency of 6.6%. Temperature dependence of the open circuit voltage (V_{oc}) derived from *I–V* measurements with varied temperature from $T = 10$ K to $T = 325$ K was linear in the range 250 K to 325 K (see figure 1). It is known that the temperature dependence of V_{oc} near room temperature can be presented as [16, 17]

$$V_{oc} = \frac{E_{A,V_{oc}}}{q} - \frac{nkT}{q}\ln\left(\frac{I_{00}}{I_L}\right), \tag{1}$$

where I_L, $E_{A,V_{oc}}$, n, k are the photocurrent, an activation energy, the diode ideality factor and the Boltzmann constant, respectively. The constant q is the electrical charge of the electron and I_{00} is obtained from the temperature dependence of the dark saturation current I_0. In good solar cells $-I_L \approx I_{sc}$, where I_{sc} is a short circuit current. I_0 equals [16, 17]

$$I_0 = I_{00}\exp\left(-\frac{E_{A,V_{oc}}}{nkT}\right) \approx AT^3 \cdot \exp\left(-\frac{E_{A,V_{oc}}}{nkT}\right). \tag{2}$$

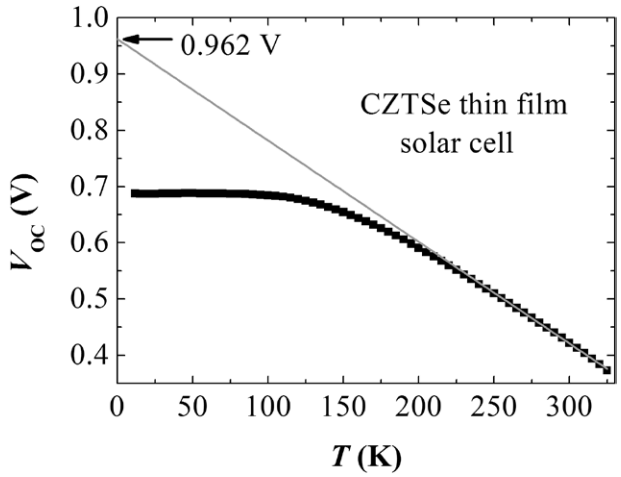

Figure 1. Temperature dependence of V_{oc} of a CZTSe thin film solar cell.

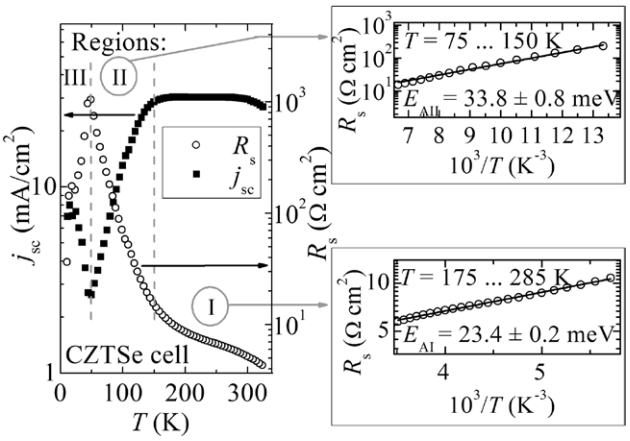

Figure 2. Temperature dependence of j_{sc}. Insets show found activation energies in region I and II.

In general, the activation energy $E_{A,V_{oc}}$ and also I_{00} depend mostly on the dominating recombination mechanism in the solar cell. In the case of bulk recombination $E_{A,V_{oc}} \approx E_g$, where E_g is the band gap energy of the absorber material.

Linear fitting of the temperature dependence of V_{oc} showed that $E_{A,V_{oc}} = 962$ meV (see figure 1), which is in good agreement with the band gap energy of CZTSe that is expected to be in the vicinity of 1 eV [4, 18], and hence the dominating recombination mechanism seems to be bulk recombination.

According to the temperature dependence of j_{sc} (see figure 2) three different temperature regions can be distinguished. Similar behaviour was also seen in CZTS [13]. At temperatures $T > 150$ K (region I) the series resistance R_s decreases with increasing temperature, indicating the thermal activation of carriers. In this region, R_s can be calculated by

$$R_S = R_{S0} \exp(E_A/kT), \tag{3}$$

where R_{s0} covers all parameters that are temperature-independent and E_A is an activation energy. Using equation (3), the activation energy $E_{AI} = 23.4 \pm 0.2$ meV was found in the temperature range 175 K to 285 K (region I). Similar values in kesterites have been published before, for example 29–48 meV [19, 20]. In our sample, the activation energy of 23.4 meV is related to grain boundaries or some shallow acceptor-like defect.

At intermediate temperatures (region II, $T = 50$ K to 150 K) another thermally activated process appears. Using equation (3), the activation energy $E_{AII} = 33.8$ meV was found in the temperature range $T = 75$ K to 150 K. In our previous studies [3, 4, 21] this activation energy was related to potential fluctuations of the valence band edge; it is the energy needed by holes to cross barriers that were created by these potential fluctuations. According to the literature, the root mean square depth of the potential well γ in CZTSe is usually in the range $\gamma = 20$–30 meV [3, 4, 21]. At the same time it is shown that in region II, the dependence of the series resistance on temperature changes and a typical Mott's variable-range hopping conduction starts to emerge [22]. This behaviour is expected in all heavily doped materials, where spatial potential fluctuations create deep potential wells for holes. But at the same time, we also expect an increasing role of bulk recombination in region II, as previously seen in CZTS [13]. At low temperatures ($T \lesssim 150$ K), the carriers, here holes, can occupy shallow acceptor states in the band gap. These states can arise from intrinsic defects or impurities or their interaction. At a sufficiently high concentration of these states, but below the critical Mott concentration, overlapping of carriers wave functions could form a so-called impurity band [23]. In such a case charge carriers can move from one shallow impurity state to another one at its spatial neighbourhood and conduction in the impurity band is expected [22]. These different processes could all be present and therefore we do not focus so much on activation energy here.

At low temperatures (region III, $T = 10$ K–50 K) the maximum of series resistance is present. By analyzing j_{sc} and I–V graphs (see figure 3), it can be seen that I–V curves have similar shapes symmetrically to both sides of 50 K. Also, impedance curves have quite similar patterns symmetrically to the temperature of $T = 50$ K in the Nyquist plot (compare the complex impedances at 10 K and 100 K in figure 4). The sudden drop in resistance below 50 K seems to be related to blocking of the interface recombination. The rapid change in the series resistance can occur because of cooling of the recombination processes: generated holes are not able to tunnel through the potential barrier into the interface region between CZTSe and CdS and therefore the interface recombination rate must be very small at these very low temperatures ($T = 10$ K–50 K) [13].

IS is a powerful non-destructive tool for characterizing semiconductors. IS detects the ac current response of a system to a small ac voltage signal with varied frequency. The impedance can be calculated by $Z = V/I$. From complex impedance the capacitance can be calculated, but this requires a certain equivalent circuit to be known. The temperature dependence of Z' and $-Z''$ of the CZTSe thin film solar cell is shown in figure 4.

Our measured impedance curves in the Nyquist plot in the whole temperature range can be fitted by applying an equivalent circuit, where a series resistor is followed by a resistor and a capacitor connected in parallel and followed by additional elements (R_{p2} and CPE) connected in parallel (circuit

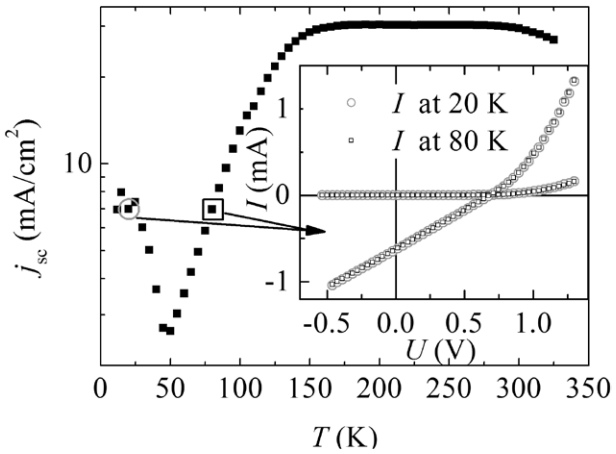

Figure 3. Temperature dependence of j_{sc}. Inset shows *I–V* curve shape similarity between both sides of 50 K at different temperatures.

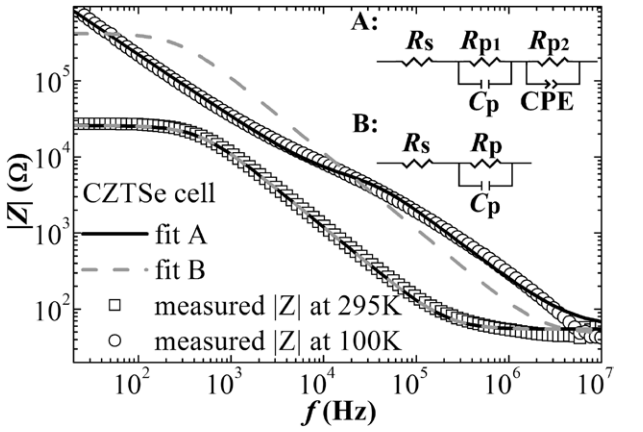

Figure 5. Measured impedance of the CZTSe solar cell and fitting results with corresponding equivalent circuits. A better fit was obtained by A. Commonly used equivalent circuit B is not suitable at lower temperatures $T \lesssim 150$ K. At room temperature no enormous difference was seen.

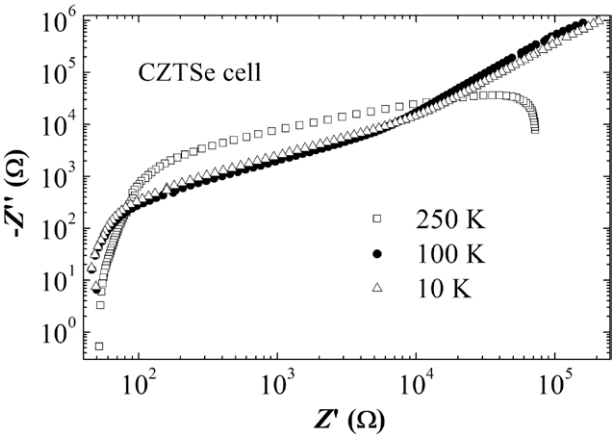

Figure 4. Nyquist plots. Selection of impedance curves of the CZTSe thin film solar cell in the logarithmic scale at temperatures 250 K, 100 K and 10 K.

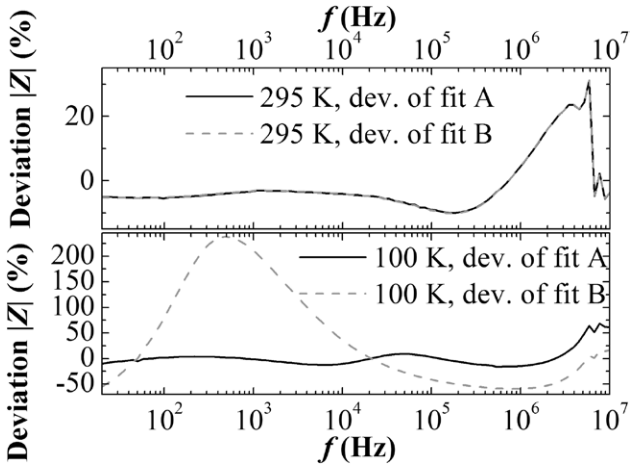

Figure 6. Fitting deviations of |Z| versus frequency at temperatures 295 K and 100 K of the CZTSe solar cell.

A in figure 5). The used complex impedance of a CPE, Z_{CPE} is given by

$$Z_{CPE} = \frac{1}{C_{CPE} \cdot (i * \omega)^P}, \tag{4}$$

where C_{CPE} is equal to capacitance C, if parameter $P = 1$. ω stands for angular frequency. But fitting of high temperature IS curves is also satisfactory with an equivalent circuit, where a series resistor is followed by a resistor and a capacitor connected in parallel (circuit B in figure 5). In figure 5 both theoretical fittings and experimental data curves are shown. In figure 6 the deviation between theoretical and experimental impedance data is shown. It is clearly seen that at room temperature there is no difference between fittings with circuits A and B, but the deviation between fitted and measured |Z| increases at higher frequencies. At low temperatures, i.e. $T \lesssim 150$ K, the equivalent circuit B was not suitable at all, and the equivalent circuit A fitting deviation of measured |Z| is enormously high (more than 50%) at quite high frequencies. Obviously, condition $R_s \ll (\omega C)^{-1}$ [10] is not satisfied at higher frequencies. It was checked by calculations and found that this condition is satisfied at frequencies $f < 3.7$ MHz at 100 K and at $f < 250$ kHz at room temperature. Moreover, measurement instrumentation capabilities have limits and affect measurements data. At low frequency, the fitting deviations of |Z| were not significant. Hence, IS results at higher frequencies are not trustworthy, and wide fitting deviations of |Z| coincide with neglecting the condition $R_s \ll (\omega C)^{-1}$.

At every measured temperature values of the equivalent circuit elements can be found by exploiting the *Z* view program for fitting. In turn, the R_s values can be used to calculate the capacitance. When assuming series inductance to be insignificant or absent, equivalent circuit B can be described by the following equation [24]:

$$Z = R_S + \frac{R_P}{1 + (\omega R_P C)^2} - i\frac{R_P^2 C\omega}{1 + (\omega R_P C)^2}, \tag{5}$$

where ω, C and R_P are angular frequency, capacitance and parallel resistance, respectively. After rewriting (5), the capacitance can be found by

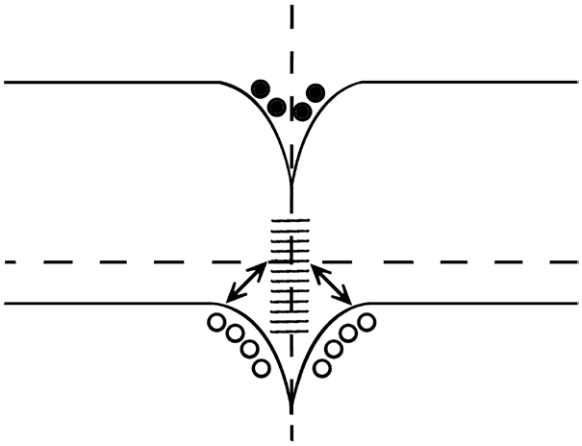

Figure 7. Grain boundary located between grains in the thin film solar cell. Some interface states are affected at quite low temperatures and these impact fittings of measured data.

$$C = \frac{-Z''}{[(Z' - R_S)^2 + (-Z'')^2] \cdot \omega}, \tag{6}$$

where Z' and $-Z''$ are the real and imaginary part of the complex impedance, respectively. Equation (6) can be used for capacitance calculation, if equivalent circuit B is applied for the fittings. In equivalent circuit A, CPE is used and in this case equations (5) and (6) would take a much more complicated form and the calculation of capacitance would not be straightforward. Thus, in the case of our studied CZTSe thin film solar cell capacitance should be derived by using equivalent circuit B and valid results are obtained only at higher temperatures ($T = 150$ K to 325 K). However, IS results are also beneficial in this low temperature range, because they add complementary or confirmative details about processes.

Temperature dependence of electrical parameters seen by IS in the CZTSe thin film solar cell at $T \lesssim 150$ K can be explained by grain boundaries, see figure 7. It seems that some interface states at grain boundaries are affected and change electrical properties of the studied cell at low temperatures. These states may not show a real capacitance, but can be explained by CPE in the equivalent circuit due to grain boundaries with different properties. This extra capacity is caused by holes being captured by interface states in grain boundaries, which are below the Fermi level, and released by states, which are above the Fermi level. If the cell is contacted and being electrically disturbed, then the band bending and hence crossing between Fermi level and interface states change. As a result, charging or discharging of these states occurs and capacitance can be detected.

As a result of this kind of capacitance change at low temperatures $T \lesssim 150$ K, where grain boundary states are affected, we need to add extra elements to our equivalent circuit. At high temperatures ($T = 150$ K–325 K), where grain boundary states do not contribute to capacitance, both equivalent circuits give excellent results. This low temperature ($T = 10$ K–150 K) behaviour, which requires the use of CPE and is present in the studied CZTSe thin film solar cells, was not seen in our previous research on monograin solar cells, where the role of grain boundaries was not so notable [7, 8].

4. Conclusions

IS and current–voltage characteristics were used for characterizing the CZTSe thin film solar cell. Different temperature ranges where electrical properties change were seen. Fittings of impedance data showed that some interface states at grain boundaries are affected at low temperatures. These states can be described by CPE in equivalent circuits due to grain boundaries with different properties. Linear fitting of temperature dependence of V_{oc} showed activation energy $E_A = 962$ meV, which is in good agreement with the band gap of CZTSe. Hence the dominating recombination mechanism seemed to be bulk recombination in the studied thin film solar cell. From temperature dependence of j_{sc} the activation energies were found. In the temperature range from 175 K to 285 K the activation energy of 23.4 meV is related to the energy needed to cross the grain boundaries or some shallow acceptor-like defect. At intermediate temperatures, from 75 K to 150 K different processes like carrier localization in potential wells, radiative recombination and Mott's variable-range hopping conduction start to come into effect, showing an activation energy of $E_{AII} = 33.8$ meV. In conclusion we have shown that temperature dependent impedance and *I–V* studies can give a valuable insight into electronic processes related to grain boundaries and interfaces in solar cells.

Acknowledgment

This work was supported by the Estonian Science Foundation grant ETF 9369, by the institutional research funding IUT 19–28 of the Estonian Ministry of Education and Research, and by FP7 project CHEETAH, EC grant agreement no. 609788, by project KESTCELLS (FP7-PEOPLE-2012-ITN-316488) and by European Regional Development Funds (ERDF, FEDER Programa Competitivitat de Catalunya 2007–2013). The authors from IREC and the University of Barcelona belong to the M-2E (Electronic Materials for Energy) Consolidated Research Group and the XaRMAE Network of Excellence on Materials for Energy of the 'Generalitat de Catalunya'. S G thanks the Government of Spain for the FPI fellowship (BES-2014–068533) and E S for the 'Ramon y Cajal' fellowship (RYC-2011–09212).

References

[1] Ito K and Nakazawa T 1988 Electrical and optical properties of stannite-type quaternary semiconductor thin films *Japan. J. Appl. Phys.* **27** 2094

[2] Lee Y S, Gershon T, Gunawan O, Todorov T K, Gokmen T, Virgus Y and Guha S 2015 $Cu_2ZnSnSe_4$ thin-film solar cells by thermal co-evaporation with 11.6% efficiency and improved minority carrier diffusion length *Adv. Energy Mater.* **5** 1401372–5

[3] Grossberg M, Krustok J, Raudoja J, Timmo K, Altosaar M and Raadik T 2011 Photoluminescence and Raman study of $Cu_2ZnSn(Se_xS_{1-x})_4$ monograins for photovoltaic applications *Thin Solid Films* **519** 7403–6

[4] Grossberg M, Krustok J, Timmo K and Altosaar M 2009 Radiative recombination in $Cu_2ZnSnSe_4$ monograins

studied by photoluminescence spectroscopy *Thin Solid Films* **517** 2489–92
[5] Oueslati S, Brammertz G, Buffiére M, Köble C, Oualid T, Meuris M and Poortmans J 2015 Photoluminescence study and observation of unusual optical transitions in $Cu_2ZnSnSe_4$/CdS/ZnO solar cells *Sol. Energy Mater. Sol. Cells* **134** 340–5
[6] Yakushev M V, Forbes I, Mudryi A V, Grossberg M, Krustok J, Beattie N S, Moynihan M, Rockett A and Martin R W 2015 Optical spectroscopy studies of $Cu_2ZnSnSe_4$ thin films *Thin Solid Films* **582** 154–7
[7] Kask E, Raadik T, Grossberg M, Josepson R and Krustok J 2011 Deep defects in Cu_2ZnSnS_4 monograin solar cells *Energy Proc.* **10** 261–5
[8] Kask E, Grossberg M, Jospeson R, Salu P, Timmo K and Krustok J 2013 Defect studies in $Cu_2ZnSnSe_4$ and $Cu_2ZnSn(Se_{0.75}S_{0.25})_4$ by admittance and photoluminescence spectroscopy *Mater. Sci. Semicond. Process.* **16** 992–6
[9] Weiss T P, Redinger A, Luckas J, Mousel M and Siebentritt S 2013 Admittance spectroscopy in kesterite solar cells: defect signal or circuit response *Appl. Phys. Lett.* **104** 202105
[10] Goodman A M 1963 Metal–semiconductor barrier height measurement by the differential capacitance method—one carrier system *J. Appl. Phys.* **34** 329–38
[11] Fernandes P A, Sartori A F, Salomé P M P, Malaquias J, da Cunha A F, Graça M P F and González J C 2012 Admittance spectroscopy of Cu_2ZnSnS_4 based thin film solar cells *Appl. Phys. Lett.* **100** 233504
[12] Friesen G, Özsar M E and Dunlop E D 2000 Impedance model for CdTe solar cells exhibiting constant phase element behaviour *Thin Solid Films* **361–362** 303–8
[13] Danilson M, Kask E, Pokharel N, Kauk-Kuusik M, Varema T and Krustok J 2015 Temperature dependent current transport properties in Cu_2ZnSnS_4 solar cells *Thin Solid Films* **582** 162–5
[14] López-Marino S *et al* 2013 ZnSe etching of Zn-Rich $Cu_2ZnSnSe_4$: an oxidation route for improved solar-cell efficiency *Chem. Eur. J.* **19** 14814–22
[15] Krustok J, Raadik T, Grossberg M, Giraldo S, Neuschitzer M, López-Marino S and Saucedo E 2015 Temperature dependent electroreflectance study of $Cu_2ZnSnSe_4$ solar cells *Mater. Sci. Semicond. Process.* **39** 251–4
[16] Krustok J, Josepson R, Danilson M and Meissner D 2010 Temperature dependence of $Cu_2ZnSn(Se_xS_{1-x})_4$ monograin solar cells *Solar Energy* **84** 379–83
[17] Rau U and Schock H W 1999 Electronic properties of Cu(In,Ga)Se_2 heterojunction solar cells—recent achievements, current understanding, and future challenges *Appl. Phys.* A **69** 131–47
[18] Raulot J M, Domain C and Guillemoles J F 2005 *Ab initio* investigation of potential indium and gallium free chalcopyrite compounds for photovoltaic application *J. Phys. Chem. Solids* **66** 2019–23
[19] Leitão J P, Santos N M, Fernandes P A, Salomé P M P, da Cunha A F, González J C, Ribeiro G M and Matinaga F M 2011 Photoluminescence and electrical study of fluctuating potentials in Cu_2ZnSnS_4-based thin films *Phys. Rev.* B **84** 024120
[20] Kosyak V, Karmarkar M A and Scarpulla M A 2012 Temperature dependent conductivity of polycrystalline Cu_2ZnSnS_4 thin films *Appl. Phys. Lett.* **100** 263903
[21] Krustok J, Josepson R, Raadik T and Danilson M 2010 Potential fluctuations in $Cu_2ZnSnSe_4$ solar cells studied by temperature dependence of quantum efficiency curves *Physica* B **405** 3186–9
[22] Mott N F 1976 Impurity band conduction. Experiment and theory the metal–insulator transition in an impurity band *J. Phys. Colloq.* **37** C4-301–6
[23] Song X, Böttger P H M, Karlsen O B, Finstad T G and Taftø J 2012 Impurity band conduction in the thermoelectric material ZnSb *Phys. Scr.* **T148** 014001
[24] Bayhan H and Kavasoğlu A S 2003 Admittance and impedance spectroscopy on Cu(In,Ga)Se_2 solar cells *Turk. J. Phys.* **27** 529–35